Fe−B Bonding in (Dibromoboryl)ferrocene: A Structural and Theoretical Investigation

Andrea Appel,[†] Frieder Jäkle,[‡] Thomas Priermeier,[‡] Rochus Schmid,[‡] and Matthias Wagner*,[‡]

Institut für Anorganische Chemie der Ludwig-Maximilians-Universität München, Meiserstrasse 1, D-80333 München, Germany, and Anorganisch-chemisches Institut der Technischen Universität München, Lichtenbergstrasse 4, D-85747 Garching, Germany

Received September 19, 1995[⊗]

The geometry and electronic structure of borylferrocenes, $FcBR_2$, have been investigated by X-ray structure analysis (R = Br) and density functional theory (DFT) calculations (R = H). An interaction between filled d-type orbitals at iron and the empty p orbital of boron causes bending of the BR_2 substituent toward the central iron atom. The dip angle α* is 17.7° (18.9°) for $FcBBr_2$ (X-ray structure). Slightly larger values were calculated for the sterically unhindered model system $FcBH_2$ (α* = 21.6° [LDA/NL]). According to the DFT calculations, the Fe−B interaction in $FcBH_2$ is considerably weaker than the $Fe-C_{exo}$ bond of the isoelectronic cation $FcCH_2^+$ (α* = 41.0° [LDA/NL]). In 1,1′-diborylated ferrocene no energetically preferred rotamer was detected by our DFT calculations.

Introduction

Ferrocenyl carbocations ($FcCR_2^+$; Fc = ferrocenyl) are remarkably stable species, and the mechanism of carbenium center stabilization by the metal complex fragment has been thoroughly investigated.[1] Very little information is available about the structural and electronic properties of the analogous 1,1′-dications,[2−4] and the 1,1′,3,3′-tetracations are completely unknown. Research in this area is severely hampered by the significantly diminished stability of the 1,1′-dications compared to the monocations. The permethylated 1,1′-$[(C_5Me_4CH_2)_2Fe]^{2+}$, for example, was generated from decamethylferrocene in about 2% yield. The molecule was monitored by NMR spectroscopy at low temperatures after its *in situ* generation in a superacid medium. Only a mixture of 1,1′-$[(C_5Me_4CH_2)_2Fe]^{2+}$ with the isomeric dication 1,2-$[(C_5Me_5)C_5Me_3(CH_2)_2Fe]^{2+}$ could be obtained. Decomposition was observed at temperatures higher than −30 °C.[2] It is therefore questionable, whether 1,1′,3,3′-tetracations can be synthesized at all.

One way to circumvent this problem is to switch from the cationic methylium group (CR_2^+) to the isoelectronic uncharged BR_2 substituent. The resulting compounds with R = Br ((dibromoboryl)ferrocene,[5] **1**-Br; 1,1′-bis(dibromoboryl)ferrocene,[6] **2**-Br; 1,1′,3,3′-tetrakis(dibromoboryl)ferrocene,[7] **4**-Br) are readily available and can be handled without problems using conventional inert-gas techniques. The molecular structures of **2**-Br and **4**-Br in the solid state have recently been published by Wrackmeyer[8] and Nöth.[7] In this paper we report on the X-ray structural investigation of the missing (dibromoboryl)ferrocene (**1**-Br; Chart 1).

Chart 1. Schematic Drawings of Molecules 1−7

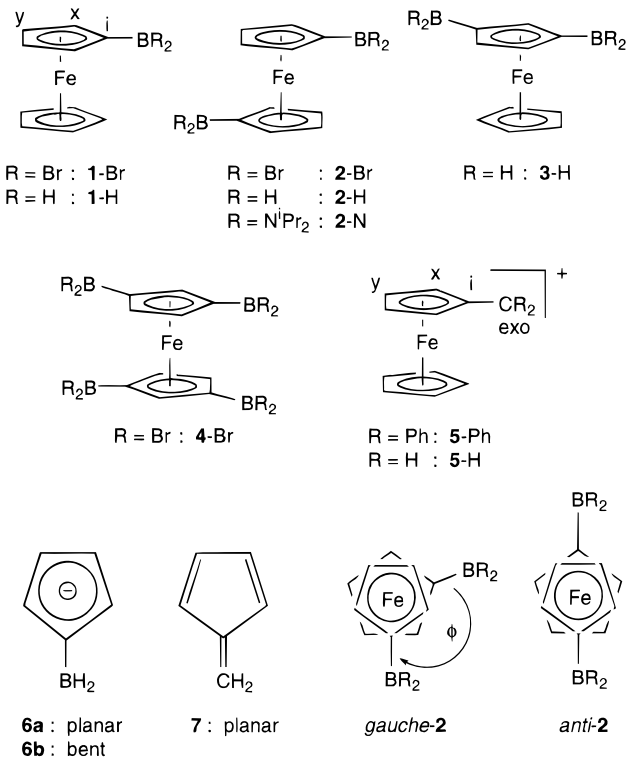

The electronic structure of the ferrocenylmethylium cation has been described as that of a fulvene−cyclopentadienyliron cation with the fulvene exocyclic double bond bent toward the iron center.[9] The principal questions are whether the isoelectronic ferrocenylborane **1** has a similar nature, how the Fe−B interaction differs

* To whom correspondence should be addressed: telefax, +49-89-32093473; e-mail, wagner@zaphod.anorg.chemie.tu-muenchen.de.
† Ludwig-Maximilians-Universität München.
‡ Technischen Universität München.
⊗ Abstract published in *Advance ACS Abstracts,* January 15, 1996.

(1) Watts, W. E. *J. Organomet. Chem. Libr.* **1979**, *7*, 399.
(2) Rybinskaya, M. I.; Kreindlin, A. Z.; Petrovskii, P. V.; Minyaev, R. M.; Hoffmann, R. *Organometallics* **1994**, *13*, 3903.
(3) Kreindlin, A. Z.; Fedin, E. I.; Petrovskii, P. V.; Rybinskaya, M. I.; Minyaev, R. M.; Hoffmann, R. *Organometallics* **1991**, *10*, 1206.
(4) Pittman, C. U. *Tetrahedron Lett.* **1967**, 3619.
(5) Renk, T.; Ruf, W.; Siebert, W. *J. Organomet. Chem.* **1976**, *120*, 1.
(6) Ruf, W.; Renk, T.; Siebert, W. *Z. Naturforsch.* **1976**, *31B*, 1028.
(7) Appel, A.; Nöth, H.; Schmidt, M. *Chem. Ber.* **1995**, *128*, 621.
(8) Wrackmeyer, B.; Dörfler, U.; Milius, W.; Herberhold, M. *Polyhedron* **1995**, *14*, 1425.
(9) Watts, W. E. *J. Organomet. Chem.* **1981**, *220*, 165.

0276-7333/96/2315-1188$12.00/0

from the Fe−C_{exo} interaction, and which effects can be observed when additional BR_2 centers are introduced into the ferrocene core. In addition to the experimental structural data, theoretical calculations provide an excellent tool to investigate these problems. We have therefore calculated the geometry and electronic structure of $FcBH_2$ (**1**-H), 1,1′-$Fc(BH_2)_2$ (**2**-H), and 1,3-$Fc(BH_2)_2$ (**3**-H) and of the related ferrocenylmethylium cation $FcCH_2^+$ (**5**-H) using density functional (DF) methods[10,11] (Chart 1). We will employ the dip angle α*, which is defined as the angle between the center of gravity of the substituted cyclopentadienyl ring, the *ipso* carbon atom, and the exocyclic carbon (boron) atom, to measure the degree of substituent bending in **1**−**5**. The aim is to learn which value of α* could be expected in the sterically unperturbed parent molecules, which molecular orbitals are responsible for Cp−BR_2 bending, and whether increased barriers to internal cyclopentadienyl rotation are found in multiply borylated ferrocenes.

Experimental Section

Synthesis of 1-Br.[5,12] **1**-Br was synthesized by direct borylation of ferrocene with BBr_3 in refluxing hexane.

X-ray Structure of 1-Br.[13] A red crystal of **1**-Br was selected in a perfluorinated oil and mounted in a glass capillary on an automatic four-circle diffractometer (CAD4, Enraf Nonius). Final lattice parameters were obtained by least-squares refinement of 25 high-angle reflections (graphite monochromator, λ = 0.710 73 Å, Mo Kᾱ). There are two crystallographically independent molecules in the asymmetric unit. Data were collected using the ω-scan method; the maximum acquisition time was 60 s for a single reflection. Data were corrected for Lorentz and polarization terms;[14,15] an absorption correction was applied according to ψ-scan data (transmission range 33.25−99.77%). For refinement, 3611 independent reflections with $I > 0.01\sigma(I)$ were used. The structure was solved by the Patterson method[16] and refined with standard difference Fourier techniques.[17] All non-hydrogen atoms were refined freely with anisotropic temperature factors; all hydrogen atoms were located in difference Fourier maps and refined isotropically. The weighting scheme of Tukey and Prince[18] was used (2 parameters): 11.1 data per parameter, shift/error <0.001 in the last cycle of refinement, residual electron density +0.67 e Å^{-3} (78 pm near Br3), −0.86 e Å^{-3}, R = 0.043, R_w = 0.039, function minimized $\sum w(|F_o| - |F_c|)^2$. Final calculations were carried out with the "PLATON"[19] program.

Theoretical Calculations. All quantum-mechanical calculations are based on density functional theory (DFT)[10,11] and were carried out on a Cray Y-MP supercomputer with the program DGauss[20] and the UNICHEM[21] interface. The DGauss program solves the Kohn−Sham equations[22] by employing Gaussian-type basis sets (LCGTO) and fits the electron density and the exchange-correlation potential to sets of auxiliary Gaussian-type functions.[11,20] Development and applications of density functional calculations have recently been reviewed by Ziegler,[23] who points out that the accuracy of DFT methods, particularly for transition-metal compounds where correlation effects are known to be important, is comparable to the much more time-consuming post-Hartree−Fock *ab initio* methods.

In this study an all-electron basis set of double-ζ plus polarization quality (DZVP) was used for all atoms, which has been especially optimized for DFT calculations, together with the A1 set of fitting functions.[24] We did not use the pseudopotential available in DGauss[25] for the iron atom, since it treats only the valence electrons explicitly and thus would fail to account for the relaxation of subvalence shells, known to be important for elements of the first transition series.[26] The use of double-ζ basis functions as opposed to using triple-ζ basis functions on the metal center was validated by fully optimizing the geometries of **1**-H and *anti*-**2**-H (Chart 1), both with a DZVP basis set and a basis set of triple-ζ plus polarization quality (TZVP)[27] on the iron atom. The differences in the geometries obtained on the DZVP- and the TZVP level are very small. For example, the most sensitive parameter, the dip angles α*, changed less than 1°. Moreover, all single-point calculations were performed on both levels of theory. Differences in DZVP and TZVP single-point energies were found to be generally smaller than 0.3 kcal/mol. Therefore, only results obtained with the DZVP basis set are discussed in this paper.

All parameters determining e.g. the grid resolution for the numerical integrations were set to the values suggested by Andzelm[20] for the DZVP basis set (DZVP level). The geometries were fully optimized without symmetry constraint on the LDA and LDA/NL level of theory until all components of the gradient were below a threshold of 0.0008 au (DZVP level). While LDA functionals are known to often overestimate bond energies, the gradient-corrected functionals (LDA/NL) reproduce the structural parameters of transition-metal compounds very accurately.[11,23,28] Consequently, the dip angle α* of the BH_2 moiety is generally found to be too large on the LDA level, whereas a self-consistent account for density gradient corrections (LDA/NL level) leads to values which are in good agreement with the experimental findings.[29] However, the differences in the calculated α* values on both levels of theory are unusually high (see Table 3), thereby indicating that the potential energy surface of **1** is very shallow with respect to changes in α*.

For a discussion of different ways to include gradient corrections to the exchange and correlation functionals, see ref 30−32. We have chosen Becke's[33] gradient-corrected functional to electron exchange and Perdew's[34] corrected functional to electron correlation, which are included self-consistently.

(10) Parr, R. G., Yang, W., Eds. in *Density Functional Theory of Atoms and Molecules*; Oxford University Press: New York, 1989.
(11) Labanowski, J. H.; Andzelm, J. W., Eds. in *Density Functional Methods in Chemistry*; Springer: New York, 1991.
(12) Wrackmeyer, B.; Dörfler, U.; Rinck, J.; Herberhold, M. *Z. Naturforsch.* **1994**, *49B*, 1403.
(13) Further details of the crystal structure investigation are available on request from the Fachinformationszentrum Karlsruhe, Gesellschaft für wissenschaftlich-technische Information mbH, D-76344 Eggenstein-Leopoldshafen, Germany, on quoting the depository number CSD 59302, the names of the authors, and the literature citation.
(14) Cromer, D. T. *International Tables of X-Ray Crystallography;* Kynoch Press: Birmingham, England, 1974; Vol. IV, Table 2.2B.
(15) Cromer, D. T. *International Tables of X-Ray Crystallography;* Kynoch Press: Birmingham, England, 1974; Vol. IV, Table 2.3.1.
(16) Sheldrick, G. M. SHELXS-86; Universität Göttingen, Göttingen, Germany, 1986.
(17) Watkin, D. J.; Betteridge, P. W.; Carruthers, J. R. *CRYSTALS*; Oxford, England, 1986.
(18) Prince, E. *Mathematical Techniques in Crystallography*, Springer-Verlag: Berlin, 1982.
(19) Spek, A. L. The EUCLID Package. In *Computational Crystallography*; Sayre, D., Ed.; Clarendon Press: Oxford, England, 1982.
(20) Andzelm, J.; Wimmer, E. *J. Chem. Phys.* **1992**, *96*, 1280.
(21) UNICHEM 2.3, Cray Research, Inc., **1994**.
(22) Kohn, W.; Sham, L. J. *Phys. Rev. A* **1965**, *140*, 1133.
(23) Ziegler, T. *Chem. Rev.* **1991**, *91*, 651.
(24) Godbout, N.; Salahub, D. R.; Andzelm, J.; Wimmer, E. *Can. J. Chem.* **1992**, *70*, 560.
(25) Chen, H.; Krasowski, M.; Fitzgerald, G. *J. Chem. Phys.* **1993**, *98*, 8710.
(26) Hay, P. J.; Wadt, W. R. *J. Chem. Phys.* **1985**, *82*, 270.
(27) Schäfer, A.; Huber, C.; Ahlrichs, R. *J. Chem. Phys.* **1994**, *100*, 5829. The triple-ζ basis set is augmented with two diffuse p-type functions (0.2/0.06), as supplied by the DGauss 3.0 file of basis sets.
(28) Jones, R. O.; Gunnarsson, O. *Rev. Mod. Phys.* **1990**, *61*, 689.
(29) Mlynarski, P.; Salahub, D. R. *Phys. Rev. B* **1991**, *43*, 1399.
(30) Fan, L.; Ziegler, T. *J. Chem. Phys.* **1991**, *94*, 6057.
(31) Fan, L.; Ziegler, T. *J. Chem. Phys.* **1991**, *95*, 7401.
(32) Lee, C.; Fitzgerald, G.; Yang, W. *J. Chem. Phys.* **1993**, *98*, 2971.
(33) Becke, A. D. *Phys. Rev. A* **1988**, *38*, 3098.
(34) Perdew, J. P. *Phys. Rev. B* **1986**, *33*, 8822.

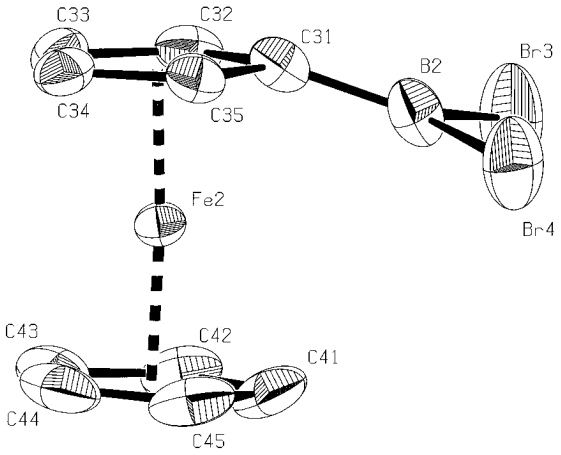

Figure 1. Molecular structure of **1**-Br_B (thermal ellipsoids at 50% probability level). Hydrogen atoms are omitted for clarity. Important structural features (COG = center of gravity of the Cp ring): Fe2···B2, 2.840 Å; Cp,Cp′ tilt angle COG−Fe2−COG′, 175.9°; Cp,Cp′ conformation C31−COG−COG′−C41, 1.6°.

Table 1. Summary of Crystallographic Data for the Complex 1-Br

compd	**1**-Br
formula	$C_{10}H_9BBr_2Fe$
fw	355.7
cryst dimens, mm	0.64 × 0.72 × 0.26
cryst syst	triclinic
space group	$P\bar{1}$
temp, K	223
a, Å	8.188(1)
b, Å	11.472(2)
c, Å	12.420(2)
α, deg	94.06(1)
β, deg	96.65(1)
γ, deg	102.84(1)
V, Å^3	1124(1)
D_{calc}, g cm^{-3}	2.101
Z	4
radiation	Mo Kα̃, 0.710 73 Å
no. of total rflns	4244
no. of obsd rflns	3611
no. of params	325
μ, cm^{-1}	84
final *R*	0.0427
final R_w	0.0387

Results and Discussion

Structural Features of Molecules 1−5. (Dibromoboryl)ferrocene (**1**-Br; Table 1) crystallizes from hexane as cherry red crystals in the space group $P\bar{1}$ with two crystallographically independent molecules in the asymmetric unit (**1**-Br_A, **1**-Br_B; see Figure 1). Selected bond lengths, angles, and dihedral angles of both molecules are given in Table 2. The complete set of structural data for **1**-Br_A and **1**-Br_B is available on request.[13]

The most peculiar feature of the molecular structure of **1**-Br is the remarkable bending of the BBr_2 substituent toward the central iron atom, which has also been observed in the analogous ferrocenyl derivatives bearing two (**2**-Br) and four (**4**-Br) BBr_2 substituents. We employed the angle α* between the center of gravity (COG) of the substituted cyclopentadienyl ring, the *ipso* carbon atom C_i, and the boron atom to measure the degree of Cp−BBr_2 bending, because α* is only slightly influenced by Cp ring puckering. For any reference molecule, for which the value of α* was not given by the authors of the original papers, we have calculated α* from the deposited atomic coordinates.[35] A comparison of important geometrical parameters of the molecules **1**−**5** is given in Tables 3 and 4.

Table 2. Selected Bond Distances (Å) and Angles (deg) and Dihedral Angles (deg) for the Compound 1-Br

	1-Br_A		
B(1)−C(11)	1.482(8)	C(12)−C(13)	1.410(8)
B(1)−Br(1)	1.916(6)	C(13)−C(14)	1.409(8)
B(1)−Br(2)	1.947(6)	C(14)−C(15)	1.414(8)
C(11)−C(12)	1.453(7)	C(11)−C(15)	1.445(7)
C(11)−B(1)−Br(1)	123.3(4)	C(12)−C(11)−B(1)	124.2(5)
C(11)−B(1)−Br(2)	120.8(4)	C(15)−C(11)−B(1)	125.2(5)
Br(1)−B(1)−Br(2)	115.9(3)	C(12)−C(11)−C(15)	106.5(5)
C(13)−C(12)−C(11)−B(1)	158.6	C(14)−C(15)−C(11)−B(1)	−158.0
Br(1)−B(1)−C(11)−C(12)	9.0	Br(2)−B(1)−C(11)−C(15)	−18.4
	1-Br_B		
B(2)−C(31)	1.474(9)	C(32)−C(33)	1.404(8)
B(2)−Br(3)	1.945(7)	C(33)−C(34)	1.411(8)
B(2)−Br(4)	1.921(7)	C(34)−C(35)	1.402(8)
C(31)−C(32)	1.455(8)	C(31)−C(35)	1.457(7)
C(31)−B(2)−Br(3)	121.8(5)	C(32)−C(31)−B(2)	126.0(5)
C(31)−B(2)−Br(4)	121.8(5)	C(35)−C(31)−B(2)	124.5(5)
Br(3)−B(2)−Br(4)	116.3(4)	C(32)−C(31)−C(35)	104.7(5)
C(33)−C(32)−C(31)−B(2)	156.2	C(34)−C(35)−C(31)−B(2)	−156.9
Br(3)−B(2)−C(31)−C(32)	17.3	Br(4)−B(2)−C(31)−C(35)	−14.5

Table 3. Comparison of Selected Experimental and Theoretical Data for the Monosubstituted Ferrocenes 1 and 5

		1-H			**5**-H	
	1-Br X-ray	LDA/NL	LDA	**5**-Ph X-ray	LDA/NL	LDA
α* (deg)[a]	A: 17.7[b] B: 18.9	21.6	32.6	21.1	41.0	44.3
ϕ (deg)[c]	A: 6.6 B: 1.6	0.4	0.8	9.5	0.0	0.0
*γ** (deg)[d]	A: 175.3 B: 175.9	177.0	176.6	169.0	167.4	166.7
Cp−B/C (Å)	A: 1.482 B: 1.474	1.525	1.514	1.417	1.405	1.402
Σ (deg)[e]	A: 360 B: 360	360	360	359	358	357
LOW[f]						
Fe		−0.44	−0.48		−0.44	−0.48
B/C_{exo}		−0.32	−0.40		−0.22	−0.24
MBO[g]						
Fe−B/C_{exo}		0.17	0.25		0.56	0.60

[a] α* = COG−C_i−(B/C_{exo}). [b] A and B refer to two crystallographically independent molecules. [c] *ϕ* = deviation from staggered conformation. [d] *γ** = COG−Fe−COG′. [e] Σ = Sum of angles around B/C_{exo}. [f] LOW = Löwdin net atomic charges. [g] MBO = Mayer bond order.

According to these data Cp−BBr_2 bending is by far the greatest in **1**-Br (**1**-Br_A, α* = 17.7°; **1**-Br_B, α* = 18.9°). Only half this value is found in **2**-Br (α* = 9.1°), and in the case of **4**-Br, two different dip angles of even smaller magnitude are observed (α^*_a = 6.8°, α^*_b = 0.1°). Moreover, in 1,1′-bis[bis(diisopropylamino)boryl]ferrocene, (**2**-N), the Cp−$B(N^iPr_2)_2$ moieties are planar within experimental error.[8]

Both the X-ray structural data and the DFT calculations show **1** to possess almost parallel Cp rings; the angle between the centers of gravity of the Cp rings and the iron atom (COG−Fe−COG′) is about 176° (Table 3). With the X-ray structural data as an initial guess for

(35) Allen, F. H.; Kennard, O.; Taylor, R. *Acc. Chem. Res.* **1983**, *16*, 146.

Table 4. Comparison of Selected Experimental and Theoretical Data of the Di- and Tetrasubstituted Ferrocenes 2−4

	2-Br X-ray	**2**-H (*anti*) LDA/NL	**2**-H (*gauche*) LDA/NL	**3**-H LDA/NL	**4**-Br X-ray
α* (deg)[a]	9.1	15.4	20.3	17.1	a: 6.8[b] b: 0.1
ϕ (deg)[c]	180.0	180.0	107.7		
γ* (deg)[d]	180.0	180.0	176.5	178.2	
B−Cp (Å)	1.456	1.526	1.528	1.527	a: 1.556 b: 1.479
Σ (deg)[e]	360	360	360	360	a: 360 b: 360
LOW[f]					
Fe		−0.41	−0.44	−0.43	
B		−0.29	−0.29	−0.29	
MBO[g]					
Fe−B		0.14	0.15	0.15	

[a] α* = COG−C_i−B. [b] a and b refer to two different values in the same molecule. [c] ϕ = C_i−COG−COG′−C_i′. [d] γ* = COG−Fe−COG′. [e] Σ = sum of angles around B. [f] LOW = Löwdin net atomic charges. [g] MBO = Mayer bond order.

Table 5. Theoretical Structural Data (LDA/NL) for $[Cp-BH_2]^-$ (6), and Fulvene (7) in the Planar and Bent Conformations

	6a	**6b**	**7a**
α *(deg)[a]	0.0	20.0	0.0
Cp-B/C (Å)	1.495	1.496	1.357
C_i-C_x (Å)	1.459	1.461	1.480
C_x-C_y (Å)	1.395	1.395	1.366
C_y-C_y (Å)	1.451	1.449	1.482

[a] α* = COG−C_i−(B/C_{exo}) (fixed value in **6b**).

our calculations, **1** preserved an almost eclipsed conformation of both cyclopentadienyl rings. To keep computing time within a reasonable frame, we have not investigated whether a staggered conformation of the Cp rings leads to a decrease in energy. We assume that the Cp ring conformation has a negligible influence on the structural features under investigation in **1** and **5** (see below).

The experimentally found C_i−B bond distances of **1** (**1**-Br_A, 1.482 Å; **1**-Br_B, 1.474 Å) are in reasonable agreement with the theoretical values (**1**-H[LDA], 1.514 Å; **1**-H[LDA/NL], 1.525 Å), and in the case of **5**, the fit is even better (**5**-Ph, 1.417 Å; **5**-H[LDA/NL], 1.405 Å). The substituted Cp ring in **1** exhibits a small but significant bond alternation with longer C_i−C_x and C_y−C_y bonds and shorter C_x−C_y bonds (for the notation of Cp rings, see Chart 1). In the case of **1**-Br_B [**1**-H[LDA/NL]], the mean values are 1.456(8) [1.462], 1.411(8) [1.442], and 1.403(8) Å [1.431 Å], respectively. In contrast, the C−C bond lengths of the unsubstituted Cp ring are equal within experimental [calculational] error. A bond alternance similar to that found for the substituted Cp ring in **1** is calculated for the free ligand **6** (Table 5). The boron substituent in **1** possesses a planar coordination; the sum of angles around boron has a value of 360°, both in the crystal structure and in the calculated structures.

The Problem of Fe−B Bonding. Dip Angle α*, Bond Orders, and Atomic Charges. The experimental result that α* for a given BBr_2 substituent decreases when additional BBr_2 groups are introduced into the molecule indicates Cp−BBr_2 bending to be a consequence of an electronic interaction between boron and iron rather than a result of crystal lattice effects. This assumption is further confirmed by the molecular structure of **2**-N. Here, the electron deficiency of the boron atoms is eliminated by N−B π bonding, which leaves no space for Fe−B interactions. Consequently, no bending of the boryl substituents is observed.

In the following paragraphs, the problem of Fe−B bonding is discussed further with the help of density functional calculations. The calculated value of α* in **1**-H on the local density approximation (LDA) level (α* [LDA] = 32.6°) is larger than the values observed experimentally in **1**-Br (α* = 17.7, 18.9°). However, when nonlocal corrections to exchange[33] and correlation[34] (LDA/NL) are included self-consistently, an excellent agreement between both theory and experiment is achieved (α*[LDA/NL] = 21.6°; see also the Experimental Section). Differences between α* [LDA] and α* [LDA/NL] similar to those found for **1**-H are observed in the case of diborylated **2**-H and **3**-H. Again, the calculated value α*[LDA/NL] = 15.4° for *anti*-**2**-H is somewhat larger than the experimentally determined dip angle of 9.1° (**2**-Br). The decrease in the dip angle upon introduction of additional boryl groups into the same molecule is reproduced by both our LDA and our LDA/NL calculations (Tables 3 and 4).

When the experimental values of α* in **1**-Br and the ferrocenylmethylium cation **5**-Ph[36] are compared, the Fe−B interaction seems, at a first glance, to be of a similar magnitude compared to the Fe−C_{exo} interaction (**1**-Br, α* = 17.7, 18.9°; **5**-Ph, α* = 21.1°). However, for **5**-H a much higher value of α* is predicted by our DFT calculations (**5**-H, α*[LDA/NL] = 41.0°). This is in accord with the results of Gleiter,[37] who has previously investigated **5**-H using the extended Hückel (EHMO)[38,39] method (α*[EHMO] = 40°). The DFT results also fit nicely with the X-ray structural investigation of the sterically less hindered ruthenocene and osmocene derivatives $[C_5Me_5MC_5Me_4CH_2]^+$ (M = Ru, Os), where dip angles of 40.3 and 41.8° are observed.[40,41] In both **1**-Br and **5**-Ph steric hindrance is likely to prevent α* from adopting a larger value. Since Br−B π bonding is known to be very weak,[42] electronic substituent effects can be expected to play only a minor role in the case of **1**-Br. The same is true for **5**-Ph, where any significant charge delocalization from the phenyl substituents into the empty orbital at boron has also been excluded.[36]

The different dip angles calculated for **1**-H and **5**-H indicate the interaction between iron and the boryl group to be weaker than Fe−C_{exo} bonding. Consequently, the Mayer bond order (MBO)[43] of the Fe−C_{exo} bond is three times higher (0.56) than the MBO of the Fe−B bond (0.17). Moreover, the Fe−C_{exo} bond order is higher than the MBO values of any other Fe−C bond in **5**-H, which range between 0.37 and 0.52, thus indicating a true η^6-coordination of the Cp−CR_2 ligand. As a result, C_{exo} essentially loses its cationic nature (Löwdin atomic charge for C_{exo} −0.22). Despite the

(36) Behrens, U. *J. Organomet. Chem.* **1979**, *182*, 89.
(37) Gleiter, R.; Seeger, R. *Helv. Chim. Acta* **1971**, *54*, 1217.
(38) Hoffmann, R. *J. Chem. Phys.* **1963**, *39*, 1397.
(39) Hoffmann, R. *J. Chem. Phys.* **1964**, *40*, 2480.
(40) Yanovsky, A. I.; Struchkov, Y. T.; Kreindlin, A. Z.; Rybinskaya, M. I. *J. Organomet. Chem.* **1989**, *369*, 125.
(41) Rybinskaya, M. I.; Kreindlin, A. Z.; Struchkov, Y. T.; Yanovsky, A. I. *J. Organomet. Chem.* **1989**, *359*, 233.
(42) Muetterties, E. L. *The Chemistry of Boron and Its Compounds*; Wiley: New York, 1967.
(43) Mayer, I. *Int. J. Quantum Chem.* **1986**, *29*, 477.

Chart 2. Schematic Orbital Plots of 1-H

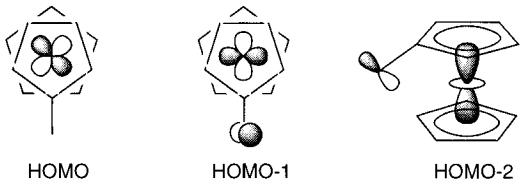

different degree of metal-to-ligand bonding in **1** and **5**, identical atomic charges for the central iron atom are calculated for both molecules (Löwdin atomic charge for Fe −0.44). This is in agreement with the Mössbauer studies of Siebert on the series of monoborylated ferrocenes $FcBX_2$ (X = F, Cl, Br, I).[44] Even though the electron-acceptor quality of the BX_2 groups differs remarkably, the same isomer shift, which is a useful probe for the charge density around iron, was found. This charge density, therefore, seems to be a poor measure for the degree of iron-to-boron/C_{exo} bonding, since the electron density that is lost by this interaction is compensated for by an increased cyclopentadienyl-to-iron charge transfer.

Further insight into the electronic structures of **1** and **2** is gained by an inspection of the influence of changes in α* on the energy of **1**-H, its Fe−B bond order, and its Löwdin charges. We have therefore calculated these parameters for selected values of α* (−21.6, 0, +21.6, +40°) at the NLDA/NL level of theory. Positive (negative) values of α* were used, when the BH_2 moiety is bent toward (away from) the central iron atom. In all four cases we have not performed a full geometry optimization, since the ferrocenyl fragment was found to be little influenced by changes in α*. Consequently, single-point calculations, which, apart from α*, employ the fully optimized LDA/NL geometry of **1**-H, can be expected to lead to reliable values in this case. It was already pointed out that the potential energy surface of **1**-H seems to be very shallow, as far as moderate changes in α* are concerned. This assumption is further confirmed by the results of the single-point calculations. Compared to the planar conformation (α* = 0°), bending of the BH_2 substituent by 21.6° away from the Fe core (α* = −21.6°) leads to an increase in energy of less than 5.5 kcal/mol, while bending by the same value in the opposite direction (optimized α*) decreases the energy of the molecule (−1.7 kcal/mol). Further bending toward the iron core, as was observed in the cation **5**-H (α* = +40°), again destabilizes **1**-H by 3.5 kcal/mol, compared to the optimized structure. The Mayer bond orders of the Fe−B bond and the electron density at boron become smaller when α* is changed from +21.6° (MBO = 0.17; LOW = −0.32) to 0° (MBO = 0.11; LOW = −0.29) and −21.6° (MBO = 0.08; LOW = −0.28). From a comparison of the energy values of **1**-H in its different conformations with dip angles of 0 and ±21.6°, the energy of this interaction may be estimated at about 7 kcal/mol.

Molecular Orbitals. An analysis of the molecular orbitals of **1**-H leads to the conclusion that the only contribution to Fe−B bonding in **1** may stem from the orbitals HOMO-1 and HOMO-2, where an overlap of the empty p orbital at boron with the $d_{x^2-y^2}$ and d_{z^2} type orbitals of the ferrocene core is possible (Chart 2). All other molecular orbitals either possess the wrong symmetry at iron or are merely ligand-centered.

Diborylated Ferrocenes. Conformations and Barriers to Internal Cyclopentadienyl Rotation. The barriers to internal rotation of the cyclopentadienyl rings in neutral ferrocenes are known to be generally very small as long as steric hindrance is absent.[45] We were interested in the question of whether this holds for 1,1′-diborylated ferrocenes as well, or whether the Fe−B donor−acceptor interaction acts as a "brake", thereby leading to a favored conformation. On the basis of NMR spectroscopic investigations and molecular orbital calculations of the extended Hückel type,[38] Rybinskaya and Hoffmann found a *gauche* conformation of both CH_2^+ centers with a dihedral angle φ of 90° to be preferred in dications of the type 1,1′-$[(C_5Me_4CH_2)_2M]^{2+}$ (M = Fe, Ru, Os)[2] (for a definition of φ see Table 4 and Chart 1). According to their calculations, only the *gauche* conformations represent minima in the rotational energy profiles, while the *syn* (φ = 0°) and *anti* rotamers (φ = 180°) correspond to maxima of the energy surfaces. These findings have been rationalized by an analysis of the molecular orbitals involved in donor−acceptor binding between iron and the carbocationic center. We will not consider further the *syn* energies of the 1,1′-dications, because these values may be severely influenced by both steric effects and electrostatic repulsion. The rotational barriers between the *gauche* and the *anti* rotamers were calculated[2] to be Δ*E*(*anti*−*gauche*) = 13.3, 15.5, and 9.4 kcal/mol for M = Fe, Ru, and Os, respectively. In the following paragraph these theoretical findings are inspected in the light of the few experimental data available and the result of our DFT calculations of **2**-H and **3**-H.

The experimentally (NMR spectroscopy) determined barrier to internal rotation of the cyclopentadienyl rings in 1,1′-$[(C_5Me_4CH_2)_2Os]^{2+}$ is 7.8 kcal/mol.[2] This value is almost identical with the one found in the parent osmocene[45] and therefore cannot be taken as a proof for any contribution of the proposed Os−C^+ donor−acceptor interaction to rotational hindrance. The X-ray structure of the 1,1′-diborylated ferrocene **2**-Br, which is isoelectronic with 1,1′-$[(C_5Me_4CH_2)_2Fe]^{2+}$, revealed an *anti* conformation of this molecule in the solid state[8] (Table 4). Furthermore, NMR spectroscopic investigations of various derivatives of **2** showed a very small barrier to internal cyclopentadienyl rotation, which is mainly caused by steric interactions.[46] The favored low-temperature conformation of compounds **2** even in solution is therefore the centrosymmetric *anti* arrangement.

To further elucidate the problem, we have done a full geometry optimization of *gauche*- and *anti*-**2**-H on the LDA as well as on the LDA/NL level. We have not found any noteworthy energy difference between the rotamers. Interestingly, the dip angle α* is nevertheless not the same in *gauche*- (α*[LDA/NL] = 20.3°) and *anti*-**2**-H (α*[LDA/NL] = 15.4°). Bearing in mind the shallowness of the potential well with respect to changes in Cp−BR_2 bending, these differences in α* are not indicative of a significantly enhanced Fe−B bond

(44) Pebler, J.; Ruf, W.; Siebert, W. *Z. Anorg. Allg. Chem.* **1976**, *422*, 39.

(45) Doman, T. N.; Landis, C. R.; Bosnich, B. *J. Am. Chem. Soc.* **1992**, *114*, 7264.

(46) Herberhold, M.; Dörfler, U.; Wrackmeyer, B. *Polyhedron* **1995**, *14*, 2683.

Chart 3. Schematic Orbital Plots of *anti*- and *gauche*-2-H

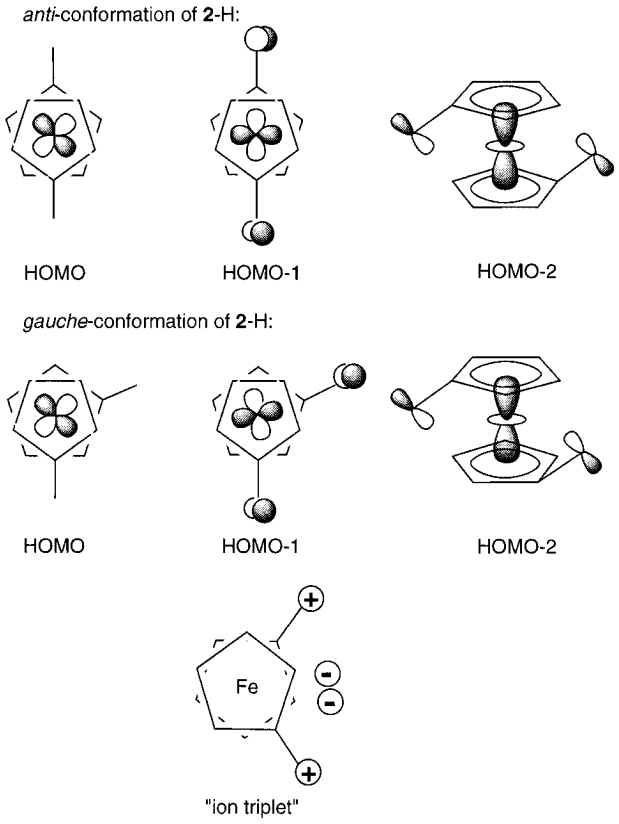

strength in *gauche*-**2**-H. The same conclusion may be drawn from a comparison of the partial charges at the exocyclic boron atoms and from an analysis of the Fe−B overlap population of both rotamers (see Table 4). As in the case of **1**-H the Fe-B interaction in *gauche*- and *anti*-**2**-H takes place in only two molecular orbitals, i.e. HOMO-1 and HOMO-2. The HOMO, which possesses mainly d_{xy} character at iron, avoids overlap with the boron acceptor (Chart 3).

The degree of the Fe−B interaction in the HOMO-1 orbital is essentially the same in *gauche*-**2**-H and in *anti*-**2**-H. The HOMO-2 orbital, which is approximately d_{z^2} at iron, does not discriminate between different rotamers as well. This different behavior between **2** and the analogous 1,1′-dications may be a consequence of the weaker Fe−B interaction compared to the Fe−C^+ interaction, as indicated by comparison of the monosubstituted specimens **1** and **5**. However, we suggest an alternative interpretation for the experimentally found preference of *gauche*-1,1′-$[(C_5Me_4CH_2)_2M]^{2+}$. When not only the cationic metallocene moiety but also the counteranions are considered, one may expect the formation of an ordered "ion triplet" at low temperatures (Chart 3). This array with the two positive and negative charges occupying opposite corners of a square is well-known, for example, in organolithium chemistry and leads to a maximization of attractive electrostatic forces.[47] This structural motif would inevitably result in a *gauche* conformation of 1,1′-$[(C_5Me_4CH_2)_2M]^{2+}$ and would not be compatible with the *anti* rotamer.

Finally, the relative energies of the 1,1′-diborylated ferrocene **2** and the 1,3-diborylated isomer **3** have been investigated. Experimentally, **2**-Br is obtained almost exclusively from the reaction of ferrocene with 2 equiv of BBr_3. However, the energy difference between **2**-H and **3**-H, calculated on the LDA/NL level, does not exceed 0.3 kcal/mol and the dip angles, as well as the Fe−B bond orders, are very similar (Table 4). The formation of **2**-Br is therefore probably a kinetically controlled reaction and has no thermodynamic reason. This conclusion is confirmed by experimental findings in the case of ruthenocene, where always a mixture of 1,3- and 1,1′-diborylated isomers is obtained.[7,8] Moreover, both dications 1,1′-$[(C_5Me_4CH_2)_2M]^{2+}$ and 1,2-$[(C_5Me_5)C_5Me_3(CH_2)_2M]^{2+}$ (M = Fe, Ru, Os) are known and have been found to possess a similar stability.[2]

Conclusion

The molecular geometry and electronic structure of borylferrocene, $FcBR_2$ (R = Br, H), have been investigated by X-ray crystallography and DFT calculations. By comparison with the ferrocenylmethylium cation $FcCR_2^+$ (R = Ph, H), as well as with di- and tetraborylated ferrocenes 1,1′-$Fc(BR_2)_2$ (R = Br, H) and 1,1′,3,3′-$Fc(BBr_2)_4$, the following conclusions can be drawn.

(a) A direct electronic interaction between d-type orbitals at iron and the empty p orbital at boron leads to bending of the exocyclic BR_2 substituent(s) toward the central iron atom. The dip angle α* possesses the largest value in $FcBR_2$ (X-ray crystallography, R = Br: α* = 17.7°, 18.9°; DFT calculations, LDA/NL level, R = H: α* = 21.6°). α* decreases continuously when additional BR_2 groups are introduced into the ferrocene core.

(b) Compared to the Fe−C_{exo} interaction in the cation $FcCH_2^+$, Fe−B bonding in $FcBH_2$ is considerably weaker as indicated by the Mayer bond orders, which are 0.56 in the former molecule but only 0.17 in the latter. Single-point calculations on $FcBH_2$ with different dip angles α* suggest the energy of the Fe−B bond to be about 7 kcal/mol.

(c) In diborylated ferrocene both conformers, *gauche*-1,1′-$Fc(BH_2)_2$ and *anti*-1,1′-$Fc(BH_2)_2$, possess the same energy. Moreover, no significant energy difference between the two isomers 1,1′-$Fc(BH_2)_2$ and 1,3-$Fc(BH_2)_2$ was found.

(d) For the theoretical treatment of ferrocenylboranes on the basis of DFT calculations, the LDA/NL level of theory, together with a basis set of double-ζ quality on all atoms (DZVP), was found to be appropriate. The LDA level is not sufficient, since it leads to an overestimation of Fe−B bonding and therefore of α*. A basis of triple-ζ quality on iron (TZVP) gave essentially the same results as the DZVP basis set.

The Fe−B interaction indicates a possibility of influencing the Lewis acidity of the boron center in ferrocenylboranes by changing the oxidation state of iron. Work is in progress in our group to exploit this feature for the design of redox-responsive hemilabile ligands[48] and of receptors for Lewis base recognition.[49]

(47) Streitwieser, A.; Swanson, J. T. *J. Am. Chem. Soc.* **1983**, *105*, 2502.

(48) Jäkle, F.; Mattner, M.; Priermeier, T.; Wagner, M. *J. Organomet. Chem.* **1995**, *502*, 123.

(49) Jäkle, F.; Priermeier, T.; Wagner, M. *J. Chem. Soc., Chem. Commun.* **1995**, 1765.

Acknowledgment. We thank Prof. Dr. W. A. Herrmann (Technische Universität München) for his generous support. Financial funding from the "Bayerischer Forschungsverbund Katalyse" (FORKAT) and the "Fonds der Chemischen Industrie" (FCI) is appreciated. We are grateful to the Leibniz Rechenzentrum, München, Germany, for providing the computational facilities and to Dr. M. Kaupp (Universität Stuttgart) for proofreading our manuscript.

Supporting Information Available: Tables giving H atom positional parameters, thermal parameters, and all bond distances and angles for **1**-Br (6 pages). Ordering information is given on any current masthead page.

OM950744Z